PNAS

Supporting Information for
KRAS mutation-driven angiopoietin 2 bestows anti-VEGF resistance in epithelial carcinomas

Kayoko Hosaka[a], Patrik Andersson[a], Jieyu Wu[a], Xingkang He[a,b], Qiqiao Du[a], Xu Jing[a], Takahiro Seki[a], Juan Gao[a], Yin Zhang[c], Xiaoting Sun[a,d], Ping Huang[e], Yunlong Yang[f], Minghua Ge[g] and Yihai Cao[a,*]

[a]Department of Microbiology, Tumor and Cell Biology, Karolinska Institute, 171 65 Stockholm, Sweden.

[b]Department of Gastroenterology, Sir Run Run Shaw Hospital, Zhejiang University School of Medicine, Hangzhou, 310016, Zhejiang, China.

[c]School of Pharmacology, Binzhou Medical University, Yantai, Shandong, 264003, China

[d]Oujiang Laboratory (Zhejiang Lab for Regenerative Medicine, Vison and Brain Health), School of Pharmaceutical Science, Wenzhou Medical University, Wenzhou 325024, China.

[e]Department of Pharmacy, Zhejiang Provincial People's Hospital, People's Hospital of Hangzhou Medical College, Hangzhou, 310053, China.

[f]Department of Cellular and Genetic Medicine, School of Basic Medical Sciences, Fudan University, Shanghai, 200032, China.

[g]Department of Head, Neck and Thyroid Surgery, Zhejiang Provincial People's Hospital, People's Hospital of Hangzhou Medical College, Hangzhou, 31003, China.

Key words: cancer, VEGF, ANG2, drug resistance, Ras mutation

*Correspondence, galley proofs and reprint requests should be primarily addressed to: Yihai Cao, M.D., Ph.D., Department of Microbiology, Tumor and Cell Biology, Karolinska Institutet, 171 65 Stockholm, Sweden. Tel: (+46)-8-5248 7596, Fax: (+46)-8-33 13 99, E-mail: yihai.cao@ki.se

This PDF file includes:

Supporting Information

SI Materials and Methods

Cell culture

A549, Calu-3, PANC1, BxPC3, HCT116, HT29, and T241 fibrosarcoma were obtained from ATCC. All purchased human cell lines including A549, Calu-3, PANC1, BxPC3, HCT116, and HT29 were de-identified at purchase. K399 cells were derived from invasive PDAC tissues of *Ptf1a*$^{cre/+}$*;LSL-Kras*$^{G12D/+}$*;Tgfbr2*$^{flox/flox}$ mice[1]. All cell lines except K399 were maintained in Dulbecco's modified Eagle's medium (DMEM, SH30243.01, HyClone) supplemented with 10% FBS. K399 cells were grown in RPMI1640 (R8758, Sigma) supplemented with 10% FBS. Cells were tested for mycoplasma contaminations, and they were negative.

Stable expression of RAS and stable knockdown of *KRAS* in tumor cell lines

pSV2 neo and pSV2 neo-hHRasG12V were kindly provided by Dr. Rak, McGill University, Montreal, Canada[2]. The full-length cDNA sequence coding for human KRas was cloned out from cDNA reverse transcripted from human MCF-7 breast cancer cell line mRNA using forward primer, 5'-atgactgaatataaacttgtg-3' and reverse primer, 5'-ttacattataatgc-3'. Site directed mutagenesis was performed to create constitutive active mutation of KRas (hKRas G12V) using normal PCR technique. Primers used are forward primer, 5'-gtggtagttggagctgttggcgtaggcaagagtg-3' and reverse primer, 5'-cactcttgcctacgccaacagctccaactaccac-3'. The amplified KRas cDNA containing point mutation was further cloned into pMXs-IG vector plasmid (kind gift from Dr. Toshio Kitamura, Tokyo University, Japan) at the Xho1/Not1 restriction site. The plasmid was verified by reading sequence.

pMXs-IG hKRas-G12V or pSV2 hHRas-G12V was transfected into T241 fibrosarcoma cell line using Lipofectamine 2000 (Invitrogen, 11668-030). Briefly, cells were seeded in a 24-well plate at 70-90% confluency. 500 ng of DNA was mixed with 2ml of Lipofectamine 2000 and Opti-MEM reduced serum medium (Gibco). After 5 min of incubation, the mixture was dropped onto the seeded cells. The transfected cells were selected either GFP positive cell sorting using FACS (FACSVantage/DiVa, BD Bioscience) or with Neomycin at 400 μg ml^{-1} concentration.

HCT116 cells seeded in a 24-well plate at 60-80% confluency were transduced with 1 μl lentivirus particles containing shRNA against human *KRAS* or control in psi-LVRU6GU (LPP-HSH088420- LVRU6GP-050, Genecopoeia). EGFP reporter signals were confirmed under fluorescence microscopy 3 days post-transduction, and successfully transduced cells were chemically selected with Puromycin at a concentration of 1-2 μg ml^{-1}. The expanded cells were checked for knockdown levels of *KRAS* and immediately injected into SCID mice.

BxPC3 cells seeded in a 24-well plate at 50-70% confluency were transduced with 50 μl lentivirus particles containing *KRAS* G12V overexpression construct (LVP1139-GP, Nucleus Biotech) or control. The transduced cells were selected with Puromycin at a concentration of 5 μg/ml, followed by cell sorting using FACS (FACSAria Fusion, BD Bioscience).

Animals, xenograft tumor models, and treatment

All mice were randomly divided into groups throughout the experiments. For murine tumor models, approximately 1-2×10^6 tumor cells in 0.05 ml of PBS were injected subcutaneously into one site in the dorsal region or two sites in the flank of each C57BL/6 mouse. Approximately 5-10 × 10^6 human tumor cells in 0.1 ml PBS were injected subcutaneously into each SCID mouse on both flanks. Tumor size was measured and the volume was calculated

using the standard formula (length × witch2 × 0.52). Tumor tissues were harvested when the tumor size reached around 0.5-1.0 cm3. In treatment experiments, tumor-bearing mice were intraperitoneally administered with a rabbit anti-mouse VEGF neutralizing antibody (2.5 mg kg−1; BD0801, Nanjing, China, kindly provided by the Simcere Pharmaceutical Company), an anti-angiopoietin 2 neutralizing antibody (MEDI3617, 10 mg kg-1, twice per week, Medimmune, kindly provided by Dr. David Jenkins) or a rat anti-mouse PDGFRβ neutralizing antibody (2C5, 40 mg kg^{-1}, twice per week, ImClone Pharmaceuticals, kindly provided by Dr. Zhenping Zhu). A rabbit nonimmune IgG (10500C; Invitrogen) or a rat nonimmune IgG (10700; Invitrogen) was used for treatments of the control group. Mice were killed by inhalation of a lethal dosage of CO2 or a high dosage of isoflurane, followed by cervical dislocation. Collected tumors were stored at -80 °C until further use or fixed in 4% PFA for the histological analysis.

Transient transfection

Tumor cells were seeded in 6 cm dishes or a 24-well plate at 50-70% confluency prior to transfection. Cells were transfected for 6-48 h in 2% FBS containing medium with small interfering RNAs targeting *KRAS* (L-005069-00-0005, Dharmacon Inc) or *FOXC2*(stB0001137A, Ribobio) using DharmaFECT transfection reagent 1 (T-2001-02, GE Healthcare). Non-specific scrambled small interfering RNAs (D-001206-14-20, Dharmacon Inc, siScrambled, siN0000001, Ribobio) were used as controls. The transfection was applied following the manufacturer's protocol (DharmaFECT; Dharmacon Inc., Ribobio). Transfected cells were further analyzed for mRNA expression and protein detection by the methods described in RNA isolation and qPCR, and Immunoblotting.

RNA isolation and qPCR

RNAs were extracted from various cultured cells using a 2-mercaptoethanol–containing lysis buffer (K7032, Thermo Scientific) or homogenized tumor tissues in TRIzol (79306, Qiagen). Purification was further performed using GeneJET RNA Purification Kits (K7032, Thermo Scientific). After measuring total RNAs with a NanoDrop 2000C Spectrophotometer (Thermo Scientific), cDNAs were synthesized using a RevertAid cDNA synthesis kit (K1632, Thermo Scientific). cDNA samples were applied to qPCR using SYBER Green master mix (4367659, Applied Biosystems) using a StepOnePlus system (Applied Biosystems). The collected data were calculated and represented as relative quantification. The specific primers used in this study included: *HRAS* forward: 5'-ATG ACG GAA TAT AAG CTG GTG GT-3'; *HRAS* reverse: 5'-GGC ACG TCT CCC CAT CAA TG-3'; *KRAS* forward: 5'-ACCTGTCTCTTGGATATTCTC-3'; *KRAS* reverse: 5'-CTGTATTGTCGGATCTCCCTC-3'; *ANGPT2* forward: 5'- TGCCACGGTGAATAATTCAG-3'; *ANGPT2* reverse: 5'-TTCTTCTTTAGCAACAGTGGG-3'; *ANGPT2* forward: 5'-AACTTTCGGAAGAGCATGGAC-3'; *ANGPT2* reverse: 5'-CGAGTCATCGTATTCGAGCGG-3'; *FOXC2* forward: 5'-GCCTAAGGACCTGGTGAAGC-3'; *FOXC2* reverse: 5'- TTGACGAAGCACTCATTGAG-3'; *ACTIN* forward: 5'-ATTGCCGACAGGATGCAGAA-3'; *ACTIN* reverse: : 5'-GCTGATCCACATCTGCTGGAA-3'; *GAPDH* forward: 5'-CATTTCCTGGTATGACAACGA-3'; *GAPDH* reverse: : 5'-GTCTACATGGCAACTGTGAG-3'; *Angpt2* forward: 5'-CCAACTCCAAGAGCTCGGTT-3'; *Angpt2* reverse: : 5'-CGGTGTTGGATGACTGTCCA-3'; *Foxc2* forward: 5'-AACCCAACAGCAAACTTTCCC-3'; *Foxc2* reverse: : 5'-GCGTAGCTCGATAGGGCAG-3'; *Pdgfb* forward: 5'-GTGTGGGCAGGGTTATTTAATATGG-3'; *Pdgfb* reverse: : 5'-

TCTTGGAGTCAAGAGAAGCCTG-3'; *36B4* forward: 5'-CGACCTGGAAGTCCAACTAC-3'; *36B4* reverse: : 5'- ATCTGCTGCATCTGCTTG

-3 ' ; *Actin* forward: 5 ' -AGGCCCAGAGCAAGAGAGG-3 ' ; *Actin* reverse: 5 ' -TACATGGCTGGGGTGTTGAA -3'.

Whole-mount staining

Tumor tissues grown in tumor-bearing mice were collected and fixed overnight with 4% paraformaldehyde (PFA). Tissues were cut into thin slices and incubated for 5 min with 20 mM proteinase K in 10 mM Tris buffer (pH 7.5). After incubation with methanol for 30 min, samples were washed twice in PBS, followed by overnight incubation with 3% skim milk in 0.3% Triton X-100 in phosphate-buffered saline (PBS). Tumor samples were incubated overnight with a rat anti-mouse CD31 antibody (1:200; 553370, BD bioscience) and a rabbit anti-mouse NG2 (1:200; Millipore, AB5320), followed by the 2h incubation of species-matched secondary antibodies including an Alexa Fluor 555-labeled goat anti-rat (1:200; A21434, Invitrogen), a Cy5-labelled goat anti-rabbit (1:200; A10523, Invitrogen), and an Alexa Fluor 647-labeled goat anti-rat (1:200; A21247, Invitrogen). After washing in PBS, samples were mounted using a Vectashield mounting medium (Vector Laboratories, Burlingame, CA, USA) and positive signals were captured using confocal microscopy (Nikon C1 Confocal microscope, Nikon Corporation, Japan) equipped with C1 software. Positive signals were further analyzed using an Adobe Photoshop software (CS5; Adobe) program. Vascular coverage was quantified as a percentage of vessels covered by $NG2^+$ cells by calculating the overlapping area of $CD31^+$ and $NG2^+$ signals.

Immunohistochemistry

PFA-fixed tumor tissues were processed for paraffin-embedding, and samples were thinly cut into 5 μm thicknesses. After baking at 60 °C, tissue slides were deparaffinized in Tissue-Clear (1466, Sakura) and rehydrated with sequential dipping in 99, 95, and 70% ethanol. Antigen retrieval procedure for 20 min incubation in a microwave, the slides were incubated in 3 % goat or donkey serum containing PBS. The slides were further stained with a rabbit anti-mouse CA9 (1:400, NB100-417, NOVUS) antibody, a rat anti-mouse Ki67 (1:200, PA5-19462, Thermo Fisher Scientific) antibody, a rabbit anti-mouse Cleaved Caspase 3 (CC3, 1:200, 9661, Cell Signaling Technology) antibody, and a goat anti-mouse CD31 (1:400, AF3628, R&D systems) antibody, a rabbit anti-mouse FSP1 (1:300, 07-2274, Merck) antibody, a mouse anti-αSMA (1:200, M0851, clone 1A4, DAKO) antibody, a rabbit anti-mouse Iba1 (1:300, 019-19741, DAKO) antibody, a rabbit anti-mouse F4/80 (1:300, 77076, Cell Signaling Technology) antibody, followed by staining with species-matched secondary antibodies including; an Alexa Fluor 555-labeled goat anti-rabbit (1:400, A21428, Invitrogen), an Alexa Fluor 555-labeled goat anti-rat (1:400, A21434, Invitrogen), an Alexa Fluor 488-labeled donkey anti-goat (1:400, A11055, Invitrogen), an Alexa Fluor 555-labeled donkey anti-rabbit (1:400, A31572, Invitrogen). In some samples, nuclei were counterstained with 4',6-diamidino-2-phenylindole (DAPI) (1:2000, D9542, Sigma-Aldrich). Positive signals were identified using a fluorescence microscope equipped with a camera (DS-Qi1MC, Nikon). Micrograph images were analyzed using Image J and Adobe Photoshop software (CS5, Adobe) programs.

H&E staining

Paraffin-embedded tissue sections rehydrated with sequential dipping in 99, 95 and 70% ethanol were stained with Hematoxylin (6765009, Thermo Fisher Scientific) and Eosin (HT110116, Sigma-Aldrich). After dehydration with sequential soaking in 95 and 99% ethanol, slides were mounted with Pertex (00801, HistoLab). Images were photographed using inverted

microscopy (Eclipse TS100, Nikon) equipped with a camera (DS-Fi1, Nikon) and software (NIS-Element F3.0, Nikon).

Blood perfusion and vascular permeability

1 mg of 2000-kDa-lysine LRD (D7139, Invitrogen) or 1.25 mg of 70-kDa-lysine LRD (D1818, Invitrogen) was injected into each mouse through the tail vein. 5 or 15 minutes after the dextran injection, mice were sacrificed by cervical dislocation. Removed tumor tissues were fixed overnight with 4% PFA and continued to whole-mount staining to visualize tumor vessels. Vessel perfusion was quantified by analyzing the vessel area containing 2000-kDa-lysine LRD per field or the perfused vessel area normalized by the vessel area. The extravasated dextran was analyzed in 70-kDa-lysine LRD region that leaked from the vessels.

ELISA

Tumor tissues were homogenized in protein lysis buffer (3228, Sigma-Aldrich) including proteinase inhibitors (1:100, 8340, Sigma-Aldrich), and used for an ELISA kit to detect human ANG2 protein levels following the manufacturer's protocol (DANG20, R&D Systems Inc.). The values were standardized by protein levels measured by BCA assay.

Immunoblotting

Various tumor cell lines seeded in a 6-well plate were incubated for 6-48 h in 2% FBS containing medium with small interfering RNAs against *KRAS* or *FOXC2*, or with various selective signaling inhibitors against MEK1/2 (U0126; 1144; Tocris Bioscience), protein kinase B (AKT inhibitor; ab142088; abcam), or NF-κB (Withaferin A; 2816; Tocris Bioscience). Non-specific scrambled small interfering RNAs or vehicle-treated tumor cells were used as a control.

Cell lysates were extracted using a Triton X-100-based lysis buffer containing proteinase inhibitors (1:100, 8340, Sigma-Aldrich) and a phosphatase inhibitor cocktail (1:100, 5870, Cell Signaling Technology). Protein concentration was measured by BCA assay. An equal amount of protein from each sample and a protein ladder (26616, Thermo Scientific) was applied to an SDS-PAGE gel (4561086/4561083, Bio-Rad), followed by wet transferring to a methanol-activated polyvinylidene difluoride membranes (IPFL00010, Millipore). Membranes were blocked at room temperature using 5% bovine serum albumin (BSA, 11413164, Fisher Scientific) in Tris borate EDTA (TBE), followed by overnight incubation with a rabbit anti-mouse ANG2 (1:1000, NBP2-67154, NOVUS) antibody, a rabbit anti-mouse FOXC2 (1:1000, 23066-1-AP, proteintech), a rabbit anti-mouse AKT (1:1000, 9272, Cell Signaling Technology), a mouse anti-phosphorylated AKT (1:1000, 4051, Cell Signaling Technology), a rabbit anti-mouse ERK (1:1000, 4695, Cell Signaling Technology), a rabbit anti-mouse phosphorylated ERK (1:1000, 9101, Cell Signaling Technology), a rabbit anti-mouse IκBα (1:1000, 4812, Cell Signaling Technology), a rabbit anti-mouse phosphorylated IκBα (1:1000, 2859, Cell Signaling Technology), or an anti-mouse β-actin antibody (1:1000, 3700, Cell Signaling Technology). Membranes were further incubated at room temperature for 60 min with a mixture of species-matched secondary antibodies, including an anti-mouse secondary antibody conjugated with IRDye 680RD (1:15000, 926-68072, LI-COR), an anti-rabbit secondary antibody conjugated with IRDye 800CW (1:15000, 926-32213, LI-COR), an anti-mouse secondary antibody conjugated with IRDye 800CW (1:15000, 926-68073, LI-COR) and an anti-rabbit secondary antibody conjugated with IRDye 680RD (1:15000, 926-32212, LI-COR). Positive signals were visualized and analyzed using an Odyssey CLx system (LI-COR).

Correlation of *ANGPT2* and *KRAS* expression in human cancer patients

KRAS mutation information and clinical information were obtained from cBioPortal (https://www.cbioportal.org)[3] and RNA-seq fragments per kilobase million (FPKM) data was obtained from The Cancer Genome Atlas (TCGA, https://cancergenome.nih.gov/) database by the TCGAbiolinks bioconductor package[4]. The expression of *ANGPT2* among 62 *KRAS* wild type and 109 mutant patients was compared using a non-parametric statistical hypothesis test, Wilcoxon signed-rank test. The correlation analysis between *KRAS* and *ANGPT2* among *KRAS* wild type and mutant patients was performed by ggstatsplot package[5]. We chose progression-free interval (PFI) as the survival outcome. The Kaplan–Meier survival of 109 PAAD, 214 CRC, and 157 LUAD patient data was conducted by R packages: "survival"[6]. The function of surv_cutpoint in R packages "survminer" was used to determine the optimal cut-off level of *ANGPT2* expression in further survival analysis[7]. All KRAS mutation subtypes are included in the study. All statistical analyses were performed by using R version 4.0.3. For all analyses. A two-tailed $P < 0.05$ was regarded as statistical significance.

SI Figures and Figure Legends

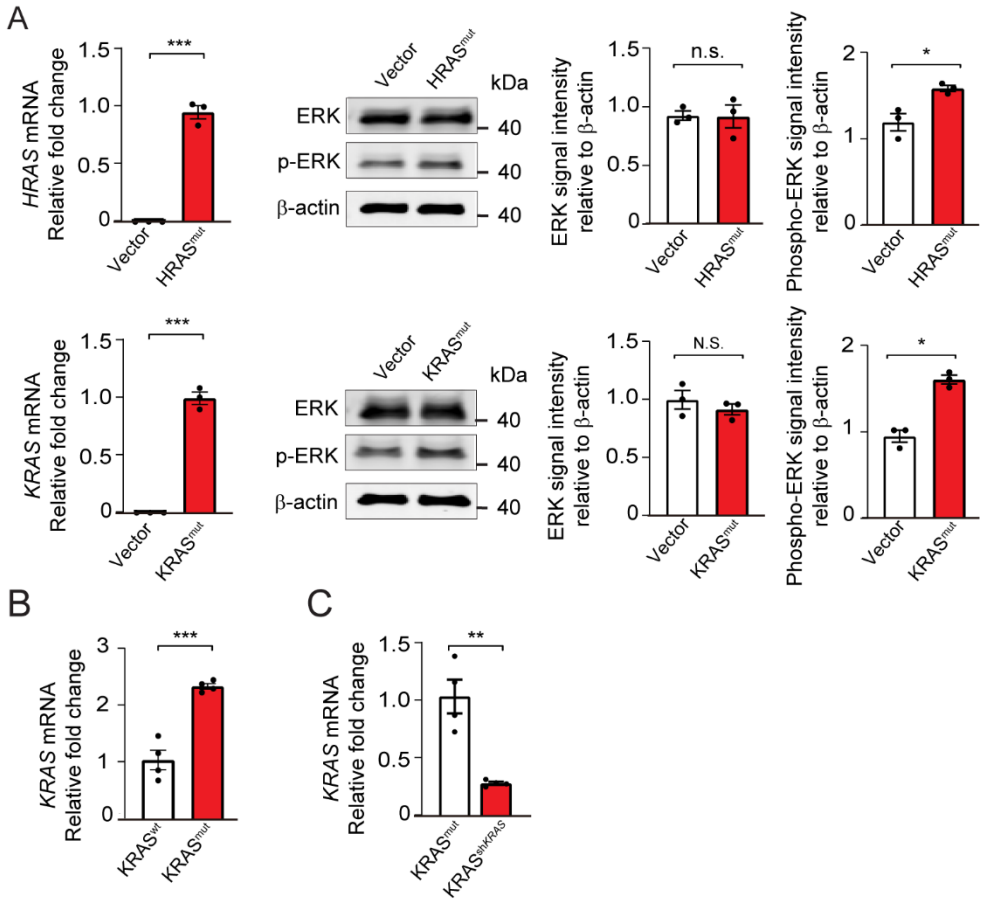

Fig. S1. Establishment of various cell lines of RAS mutant and KRAS shRNA knockdown.

(A) qPCR analysis of *HRAS* and *KRAS* mRNA expression and immunoblotting analysis of ERK and phosphorylated-ERK protein levels in T241-vector, -HRAS, and -KRAS fibrosarcoma (n = 3 samples per group).

(B) *KRAS* mRNA expression in BxPC3 PDAC KRAS wt and BxPC3 PDAC KRAS mutant tumors levels (n = 4 samples per group).

(C) *KRAS* mRNA expression in HCT116 CRC KRAS mutant and HCT116 sh*KRAS* tumors levels (n = 4 samples per group).

All data represent as mean ± s.e.m. **P* < 0.05, ***P* < 0.01, ****P* < 0.001 (two-sided unpaired *t*-test). N.S., not significant. p-ERK, phosphorylated-ERK.

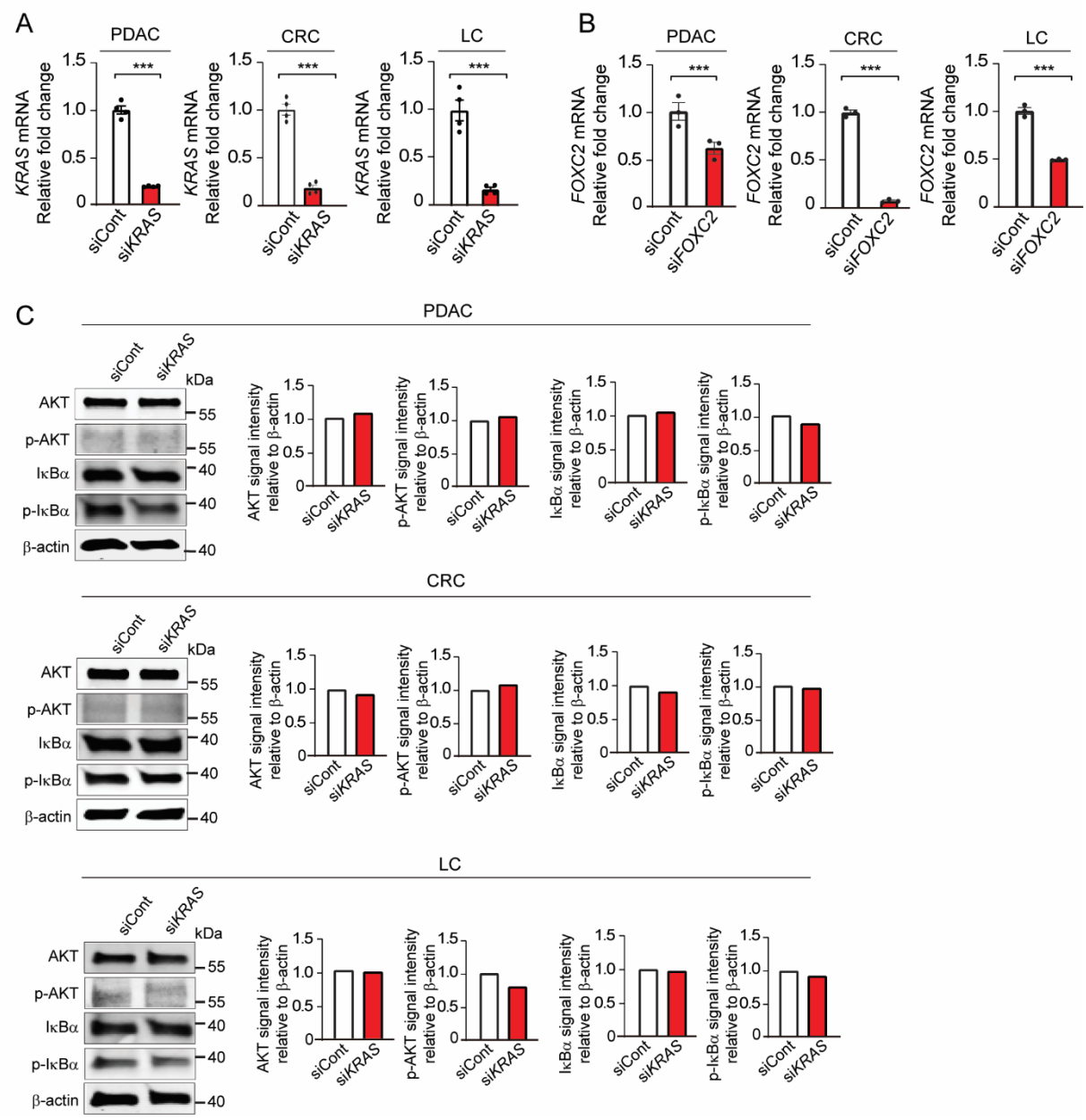

Fig. S2. Knockdown efficiency of si*KRAS*- and si*FOXC2*-RNA transfected various cell lines and signaling pathways.

(A) *KRAS* mRNA expressions in scrambled-RNA or si*KRAS*-RNA transfected PANC1 PDAC, HCT116 CRC, and A549 lung cancer cell lines (n = 4 samples per group).

(B) *FOXC2* mRNA expressions in scrambled-RNA or si*FOXC2*-RNA transfected PANC1 PDAC, HCT116 CRC, and A549 lung cancer cell lines (n = 3 samples per group).

(C) Protein expressions of AKT, phosphorylation of AKT, IκBα, and phosphorylation of IκBα in scrambled-RNA or si*KRAS*-RNA transfected PANC1 PDAC, HCT116 CRC, and A549 lung cell lines.

Data in A and B represent as mean ± s.e.m. ***$P < 0.001$ (two-sided unpaired *t*-test). N.S., not significant. p-AKT, phosphorylated-AKT; p-IκBα, phosphorylated-IκBα. PDAC, pancreatic ductal adenocarcinoma; CRC, colorectal carcinoma; LC, lung cancer.

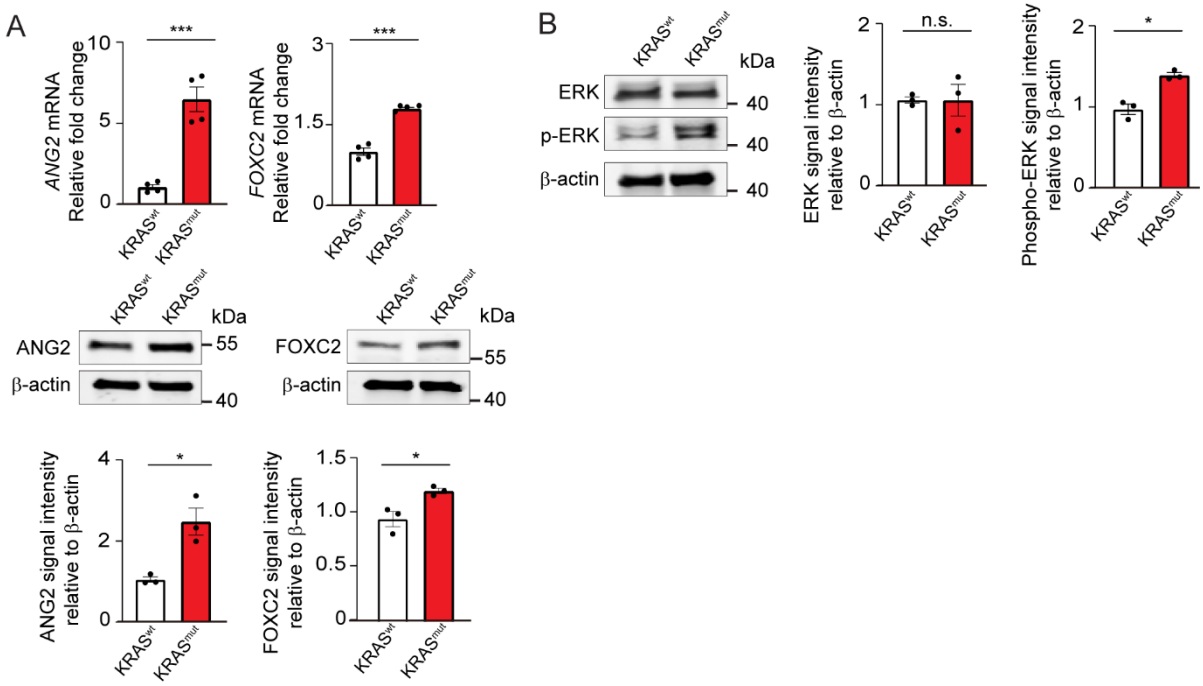

Fig. S3. Angiopoietin 2 and FOXC2 levels in BxPC3 KRAS wt and mutant cell lines.

(A) *ANGPT2* and *FOXC2* mRNA expressions in BxPC3 KRAS wt and mutant cell lines (n = 4 samples per group). ANG2 and FOXC2 protein expressions in BxPC3 KRAS wt and mutant cell lines (n = 3 samples per group).

(B) ERK and phosphorylated-ERK protein levels in BxPC3 KRAS wt and mutant cell lines (n = 3 samples per group)

All data represent as mean ± s.e.m. **P* < 0.05, ****P* < 0.001 (two-sided unpaired *t*-test). N.S., not significant. p-ERK, phosphorylated-ERK.

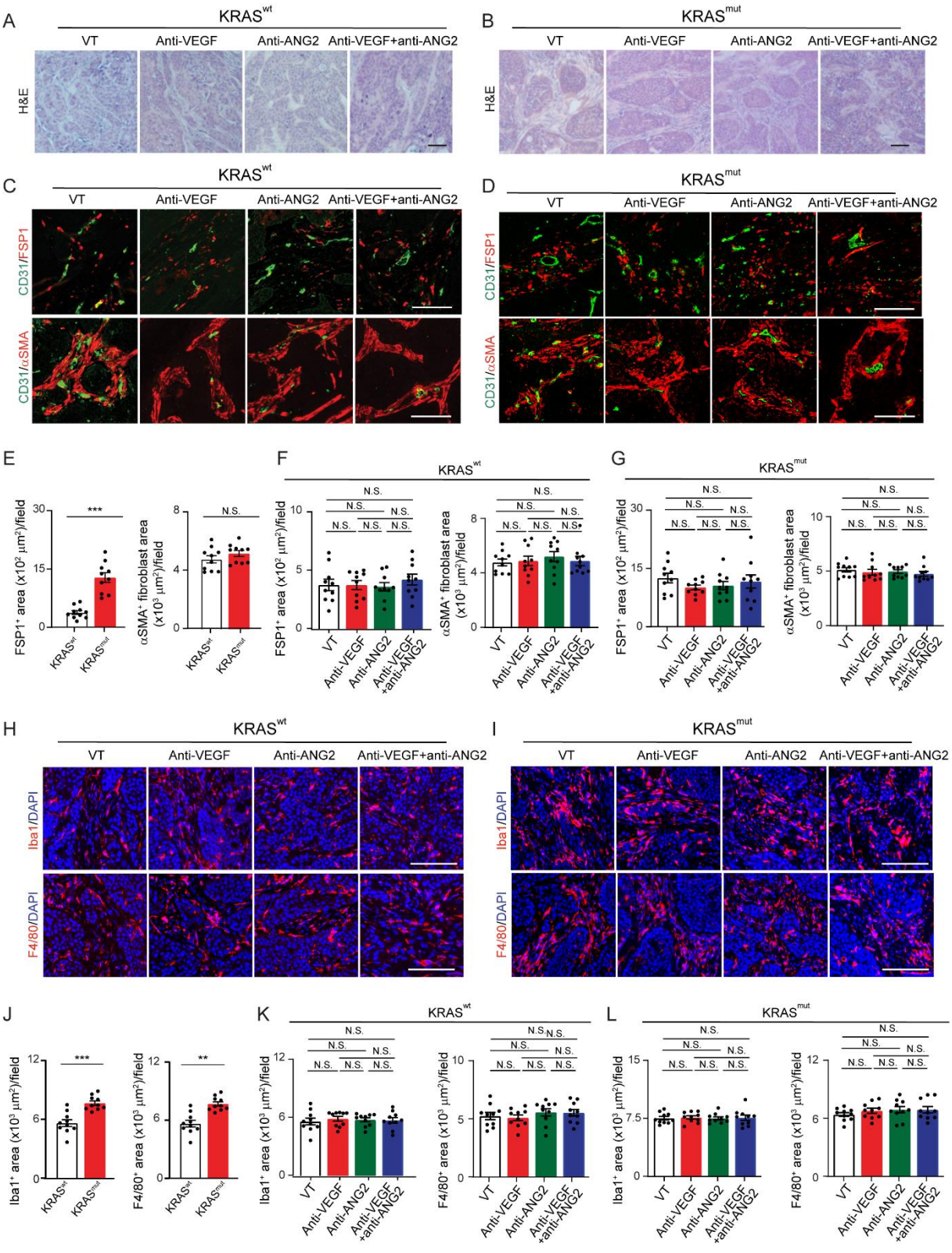

Fig. S4. Tumor stromal and macrophage components in various antibody-treated KRAS wt and mutant PDAC tumors.

(A and B) H&E staining of tumor tissues from BxPC3 KRAS wt (A) and mutant (B) tumors.

(C and D) FSP1$^+$ and αSMA$^+$ tumor-associated fibroblasts (red) in various antibody-treated BxPC3 KRAS wt (C) and mutant (D) PDAC tumors. Tumor

microvessels are stained with CD31 (green).

(E) Quantification of $FSP1^+$ and αSMA^+ signals in BxPC3 KRAS wt and mutant PDAC tumor**s** (n = 10 fields per group).

(F and G) Quantification of $FSP1^+$ and αSMA^+ signals in various antibody-treated BxPC3 KRAS wt (F) and mutant (G) PDAC tumor**s** (n = 10 fields per group). Vehicle-treated controls are the same as those in E.

(H and I) $Iba1^+$ and $F4/80^+$ tumor-associated macrophages (red) in various antibody-treated BxPC3 KRAS wt (H) and mutant (I) PDAC tumor**s**. Nuclei are counterstained with DAPI (blue).

(J) Quantification of $Iba1^+$ and $F4/80^+$ signals in BxPC3 KRAS wt and mutant PDAC tumor**s** (n = 10 fields per group).

(K and L) Quantification of $Iba1^+$ and $F4/80^+$ signals in various antibody-treated BxPC3 KRAS wt (K) and mutant (L) PDAC tumor**s** (n = 10 fields per group). Vehicle-treated controls are the same as those in J.

All data represent as mean ± s.e.m. Scale bar, 50μm. Statistical analysis was performed using two-sided unpaired *t*-tests (E and J) and one-way ANOVA followed by Tukey's multiple comparison tests (F, G, K, and L). $^{**}P < 0.01$, $^{***}P < 0.001$. N.S., not significant. DAPI, 4′,6-diamidino-2-phenylindole.

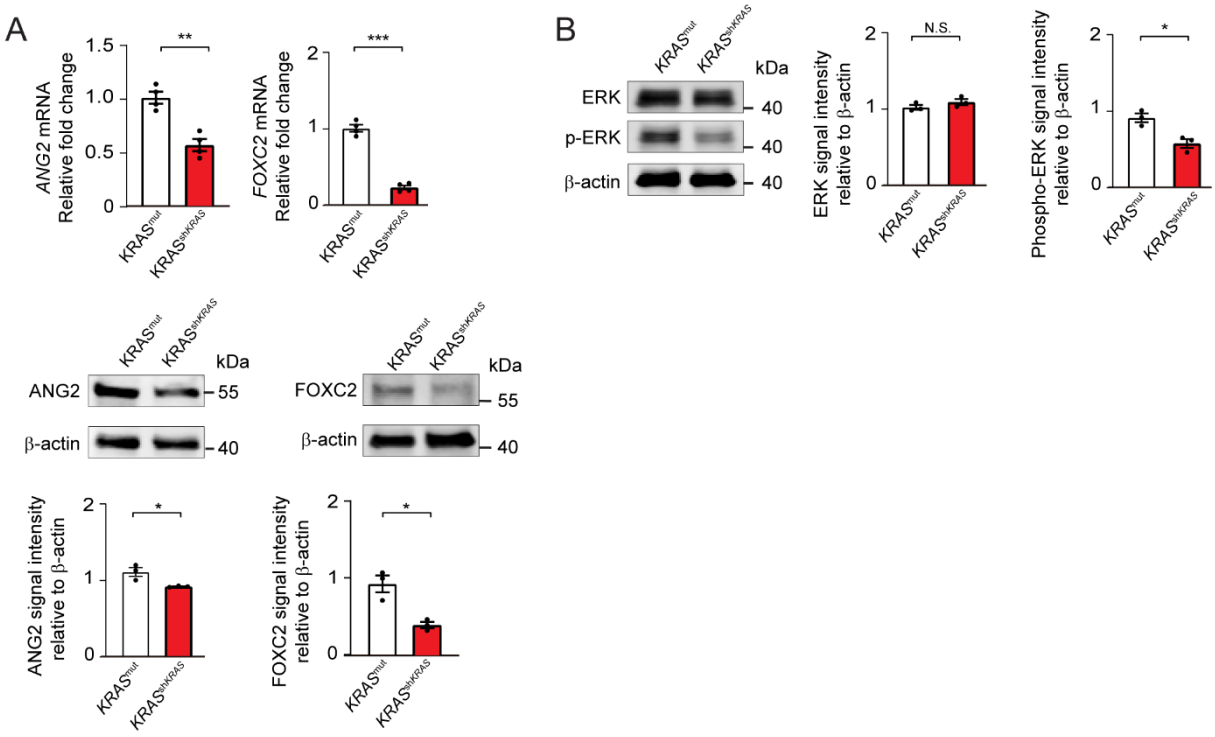

Fig. S5. Angiopoietin 2 and FOXC2 levels in HCT116 KRAS mutant and sh*KRAS* cell lines.

(A) *ANGPT2* and *FOXC2* mRNA expression levels in HCT116 KRAS mutant and sh*KRAS* cell lines (n = 4 samples per group). ANG2 and FOXC2 protein expressions in HCT116 KRAS mutant and sh*KRAS* cell lines (n = 3 samples per group).

(B) ERK and phosphorylated-ERK protein levels in HCT116 KRAS mutant and sh*KRAS* cell lines (n = 3 samples per group)

All data represent as mean ± s.e.m. **P* < 0.05, ***P* < 0.01, ****P* < 0.001 (two-sided unpaired *t*-test). N.S., not significant. p-ERK, phosphorylated-ERK.

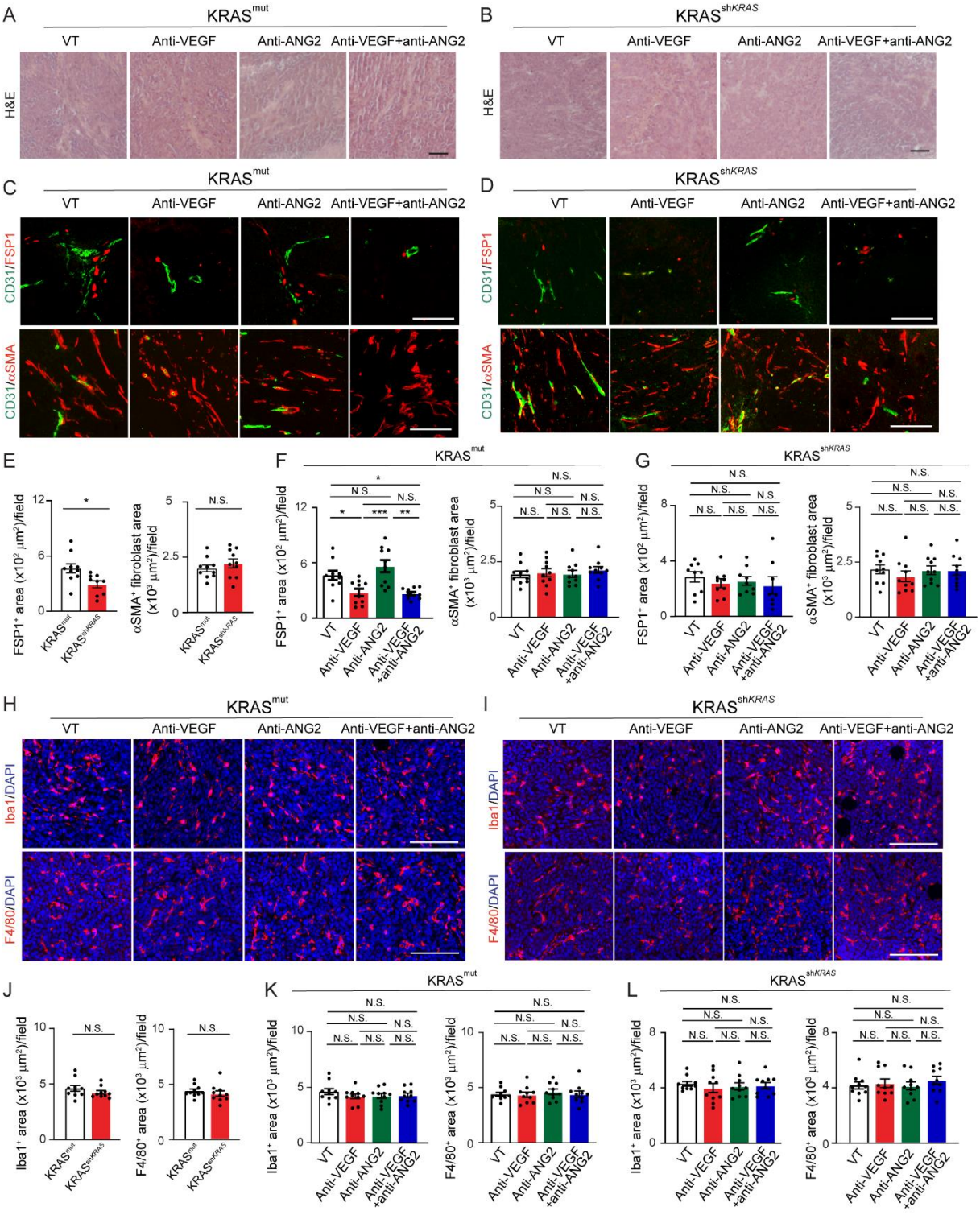

Fig. S6. The tumor microenvironment in various antibody-treated KRAS wt and mutant CRC tumors.

(A and B) H&E staining of tumor tissues from HCT116 KRAS mutant (A) and sh*KRAS* CRC tumors.

(C and D) FSP1$^+$ and αSMA$^+$ tumor-associated fibroblasts (red) in various antibody-treated HCT116 KRAS mutant (C) and sh*KRAS* (D) CRC tumors. Tumor microvessels are stained with CD31 (green).

(E) Quantification of $FSP1^+$ and αSMA^+ signals in HCT116 KRAS mutant and sh*KRAS* CRC tumors (n = 10 fields per group).

(F and G) Quantification of $FSP1^+$ and αSMA^+ signals in various antibody-treated HCT116 KRAS mutant (F) and sh*KRAS* (G) CRC tumors (n = 10 fields per group). Vehicle-treated controls are the same as those in E.

(H and I) $Iba1^+$ and $F4/80^+$ tumor-associated macrophages (red) in various antibody-treated HCT116 KRAS mutant (H) and sh*KRAS* (I) CRC tumors. Nuclei are counterstained with DAPI (blue).

(J) Quantification of Iba1+ and $F4/80^+$ signals in HCT116 KRAS mutant and sh*KRAS* CRC tumors (n = 10 fields per group).

(K and L) Quantification of Iba1+ and F4/80+ signals in various antibody-treated HCT116 KRAS mutant (K) and sh*KRAS* (L) CRC tumors (n = 10 fields per group). Vehicle-treated controls are the same as those in J.

All data represent as mean ± s.e.m. Scale bar, 50mm. Statistical analysis was performed using two-sided unpaired *t*-tests (E and J) and one-way ANOVA followed by Tukey's multiple comparison tests (F, G, K and L). $*P < 0.05$, $**P < 0.01$, $***P < 0.001$ (two-sided unpaired *t*-test). N.S., not significant.

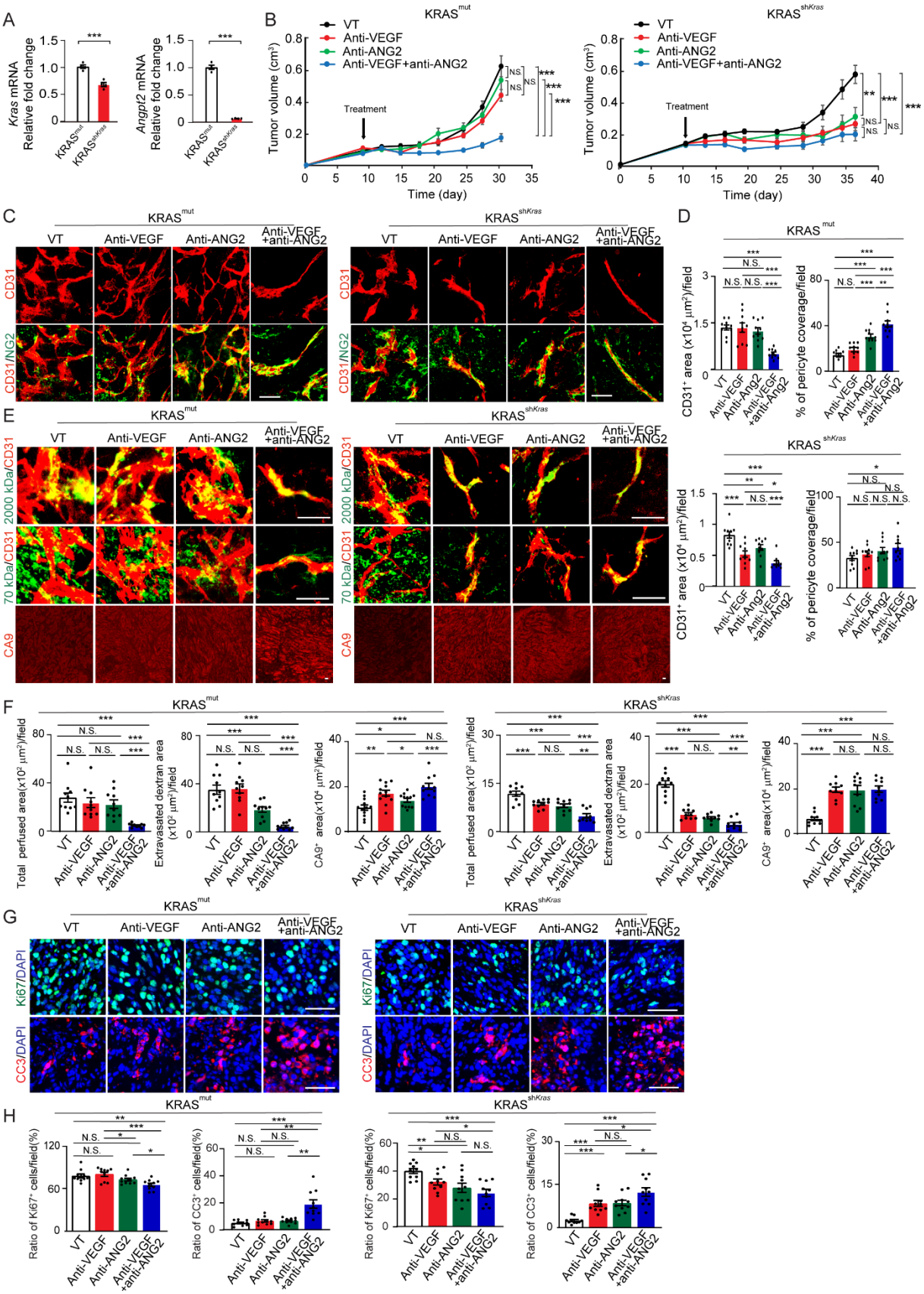

Fig. S7. Tumor growth, angiogenesis, vessel structure and anti-tumor effects in murine *Kras* mutant tumor models.

(A) *Kras* and *Angpt2* mRNA expression in K399 KRAS mutant (A) and sh*Kras* (B) PDAC tumors (n = 4 samples per group).
(B) Tumor growth rates of various antibody-treated K399 KRAS mutant and sh*Kras* PDAC tumors (n = 12-16 tumors per group).
(C) Tumor microvessels (red) and pericytes (green) in various antibody-treated K399 KRAS mutant (left) and sh*Kras*(right) PDAC tumors.
(D) Quantification of $CD31^+$ microvessels and $NG2^+$ pericyte coverage in various antibody-treated K399 KRAS mutant (upper) and sh*Kras* (lower) PDAC tumors (n= 10 fields per group).
(E) Vessel perfusion and permeability in K399 KRAS mutant (left) and sh*Kras*(right) PDAC tumors analyzed by injection of Rhodamine-labeled lysine 2000 kDa and 70 kDa dextran (green). Microvessels (red) are counterstained. $CA9^+$ signals represent hypoxia in various antibody-treated K399 KRAS mutant (left) and sh*Kras* (right) PDAC tumors.
(F) Quantification of vessel perfusion, permeability, and $CA9^+$ signals in various antibody-treated K399 KRAS mutant (left) and sh*Kras* (right) PDAC tumors (n = 10-12 fields per group).
(G) Proliferative (Ki67) and apoptotic (CC3) cell signals in various antibody-treated K399 KRAS mutant (left) and sh*Kras*(right) PDAC tumors. Nuclei are counterstained with DAPI (blue).
(H) Quantification of $Ki67^+$ proliferative and $CC3^+$ apoptotic cell signals in K399 KRAS mutant (left) and sh*KRAS* (right) PDAC tumors. (n = 10 fields per group).

All data represent as mean ± s.e.m. Scale bar, 50μm. Statistical analysis was performed using two-sided unpaired *t*-tests (A and B) and one-way ANOVA followed by Tukey's multiple comparison tests (D, F and H). **P* < 0.05, ***P* < 0.01, ****P* < 0.001. N.S., not significant. CC3, cleaved caspase 3; DAPI, 4′,6-diamidino-2-phenylindole.

SI References

1 Ijichi, H. *et al.* Aggressive pancreatic ductal adenocarcinoma in mice caused by pancreas-specific blockade of transforming growth factor-beta signaling in cooperation with active Kras expression. *Genes Dev* **20**, 3147-3160, doi:10.1101/gad.1475506 (2006).

2 Rak, J. *et al.* Oncogenes and tumor angiogenesis: differential modes of vascular endothelial growth factor up-regulation in ras-transformed epithelial cells and fibroblasts. *Cancer Res* **60**, 490-498 (2000).

3 Gao, J. *et al.* Integrative analysis of complex cancer genomics and clinical profiles using the cBioPortal. *Science signaling* **6**, pl1-pl1 (2013).

4 Colaprico, A. *et al.* TCGAbiolinks: an R/Bioconductor package for integrative analysis of TCGA data. *Nucleic acids research* **44**, e71-e71 (2016).

5 Patil, I. Visualizations with statistical details: The'ggstatsplot'approach. *Journal of Open Source Software* **6**, 3167 (2021).

6 Borgan, Ø. (Wiley Online Library, 2001).

7 Kassambara, A., Kosinski, M., Biecek, P. & Fabian, S.(2021).